Journal of International Education and Development
2026, VOL. 10, NO. 1, 158-164
DOI: 10.47297/wspiedWSP2516-250034.20261001

Flexible Coefficient Distance Regularized Level Set Evolution with Application to Image Segmentation

Ronggui Yu

Guangzhou College of Commerce, School of Information Technology & Engineering, Guangzhou, Guangdong, 511363, China

ABSTRACT

In recent years, some variational level set formulations, which are composed of a certain energy functional term and a distance regularization term(DRT), have been proposed. During the evolution of the level set function(LSF), the DRT maintains the LSF stability, eliminating the need for the complex re-initialization procedures of the traditional level set methods. The DRT should have different coefficients in different regions of the LSF. However, there is only one coefficient for the DRT of the existing re-initialization free algorithms. So we propose a flexible coefficient distance regularized level set evolution where the DRT has different coefficients in different regions of the LSF, so that the evolve rate of the LSF and image segmentation performance can be optimized. Experiments show that our algorithm has achieved good results.

KEYWORDS

Level set; Image segmentation; Re-initialize; Distance regularize; Topological changes; Boundary anti-leakage

1 Introduction

In the past three decades, a large number of research work on active contour models(ACMs) has emerged in the field of image processing and computer vision [1-2]，especially the geometric active contours(GACs) using the level set method (LSM) for image segmentation [3]. The evolving curve of the original ACMs is explicitly represented by the parametric equation，which has some inherent drawbacks [3-5], such as it is difficult to deal with topological changes and it is highly dependent on parameters. The LSM later introduced by Osher and Sethian[4, 5] overcomes the problems faced by the parametric active contour. The LSM uses a zero level set of a higher dimension to implicitly represent contour, and it transforms the motion of the contour into the evolution formulation of the level set function(LSF), the formulation is represented by a partial differential equation(PDE)[6].

The early LSM is driven by pure PDE [7], alternatively, the variational LSM uses the method of minimizing a certain energy functional, which can directly drive the evolution PDE of the LSF [8-10]. According to calculus of variation [11], when an additional information is needed to constrain the LSF, it is only necessary to add an energy functional of the additional information to the energy functional, therefore the variational LSM is more natural and convenient than the LSM driven by pure PDE.

During the evolution of the traditional level set equation, the LSF near the zero level set usually becomes very flat or steep, which leads to numerical errors and eventually destroys the stability of the evolution of the LSF. This problem has plagued the LSM that has been widely used in the fields of science and Engineering. To solve this problem, a technique called re-initialization was proposed [12-13], which periodically re-initializes the LSF to a signed distance function(SDF)[13-14]. The SDF ø has a unique characteristic $|\nabla\varnothing| = 1$, where ∇ is the gradient operator. Therefore, in many applications, the LSF is usually initialized as an SDF, and then is re-initialized as an SDF periodically during the evolution of LSF.

However, it has many problems difficult to solve for the re-initialization procedures, for example, it may incorrectly move the zero level set away from the desired location, and it does not know how and when to use the re-initialization algorithm [6].

In recent years, some level set evolution eliminates re-initialization (LSE-ER) algorithms that can automatically repair deformed LSFs during level set evolution(LSE) have been proposed, it eliminates the need of re-initialization procedure [15-18]. Firstly, Li et al. proposed a new variational formulation [16], which consists of a certain energy functional term and a newly added energy functional term. Li et al. calls the certain energy functional term as the external energy, and the newly added energy functional term as the penalty term, they all use the same LSF as the only variable. During the evolution of the LSF, the certain energy functional term drives zero level set to move towards the image target boundary, and the penalty term punishes the deviation of the LSF to the SDF. That is, the newly added penalty term will always maintain the LSF as an SDF in the whole domain, thus avoiding the re-initialization step.

However, it has a side effect that may affect the numerical accuracy, that is, the LSF surface will eventually have periodic "peaks" and "valleys". Therefore, Li et al. puts forward a distance regularization term(DRT) instead of the original penalty term, which eliminated the problems encountered in the literature [15]. Different from the penalty term that always maintain the LSF as an SDF in the whole domain, the DRT maintain the signed distance property $|\nabla\varnothing|=1$ only near the zero level set and regularize the LSF $\varnothing$ to $|\nabla\varnothing|=0$ away from the zero level set, which avoid the "peaks" and "valleys" problems.

The potential function in the DRT consists of a trigonometric function. Compared to trigonometric functions, polynomials have a simpler structure and easier to operate for function calculations, differentiations and integrations, therefore, the author in [19] uses a sixth-order Taylor polynomial to replace the trigonometric function in the double-well potential.

In order to make algorithm easier to deal with the topological changes, Xie et al. proposed another DRT which reduces the value of $|\nabla\varnothing|$ in the whole domain [17]. Xie et al. considers the risk of flattening the level set surface around zero level is very small because of the use of delta function, therefore, it is not necessary to regularize the LSF to $|\nabla\varnothing| = 1$ where $|\nabla\varnothing| < 1$. Conversely, reducing the gradient of level set surface where $|\nabla\varnothing| < 1$ can makes it more likely that the level set surface to bend over to cross zero level in order to produce new components. Recently, a re-initialization free LSE algorithm via reaction diffusion(RD) is presented [18], it consists of a reaction term and a diffusion term. The effect of this diffusion term on the LSF is similar to the above DRT, which eliminates the re-initialization procedure.

We have devised a flexible coefficient distance regularized level set evolution(FC-DRLSE) algorithm in which the coefficients of the DRT are different according to regions of the LSF. At the same time, we set the DRT coefficient in Performance-Region to a flexible coefficient whose value depends on the specific image.

In addition, we replace the sine function of the algorithm in [15] with a simpler polynomial to make the algorithm more concise and efficient in our FC-DRLSE algorithm. We apply the FC-DRLSE algorithm to composite images and real images and achieve better results than the LSE-ER algorithms described above.

The rest of this paper organized into five sections. Section 2 is a description of level set methods, re-initialization, and the LSE-ER algorithms used in this paper. In Section 3, we focus on our FC-DRLSE algorithm, experimental results shown in Section 4. Section 5 summarizes the observations and completes this paper.

2 Background and Related Works

2.1 Level Set Methods and its Re-initialization

Consider a closed dynamic contour of the parametric ACM, denoted by $C(p,t):[0,1]\times[0,\infty)\to R^2$, where a spatial parameter $p\in[0,1]$, and a temporal variable $t\in[0,\infty)$. The evolution equation of the active contour can be expressed as follows

$$\begin{cases} \dfrac{\partial C(p,t)}{\partial t} = FN \\ C(p,t=0) = C_0(p) \end{cases} \tag{1}$$

where F is the force function, N is inward normal direction of the evolution curve, and $C_0(p)$ is the initial curve. To avoid parameterization, the active contour C(p, t) can be represented by a zero level set of a LSF ø(x, y, t), that is C(t)={(x, y)| ø(C(t),t)=0}. The LSF ø takes positive values inside the zero level set and negative values outside, then its inner normal vector can be represented as $N = -\nabla\varnothing/|\nabla\varnothing|$. Therefore, Eq.(1) can be transformed into the following PDE:

$$\begin{cases} \dfrac{\partial\varnothing}{\partial t} = F|\nabla\varnothing| \\ \varnothing(x,y,t=0) = \varnothing_0(x,y) \end{cases} \tag{2}$$

which is the evolution equation of the level set.

The re-initialization equation of the standard re-initialization technique is as follows

$$\frac{\partial\varnothing}{\partial t} = s(\varnothing_0)(1-|\nabla\varnothing|) \tag{3}$$

where $ø_0$ is initial LSF, and s(ø) is the sign function.

2.2 LSE-ER

In this section, we describe five general LSE-ER algorithms. The algorithms proposed in [15-16, 19] are distance regularized level set evolution(DRLSE) algorithms, so we call them DRLSE1, DRLSE2 and DRLSE3 respectively, and we refer to these three DRLSE series algorithms as DRLSE-S. The algorithm in [17] is a constrained distance regularized level set evolution algorithm, so we call it C-DRLSE, and the algorithm in [18] is a LSE via reaction diffusion algorithm, therefore we call it LSE-RD.

2.2.1 DRLSE1

Li et al. proposed a new variational formulation which can automatically repair the LSF during the evolution of the level set [16]. The basic idea of this method is to add a penalized energy functional to the certain energy functional defined on the level set. This variational formulation is as follows

$$E(\varnothing) = E_m(\varnothing) + \mu P(\varnothing) \tag{4}$$

where μ > 0 is a constant, and $E_m(ø)$ is a certain energy functional that depends on image data, Li et al. call it the external energy. Because the penalized energy functional P(ø) is a functional of the function ø only, it is called the internal energy. This penalized energy functional as

$$P(\varnothing) = \int p_1(|\varnothing|)dxdy \tag{5}$$

where $\Omega \subset R^2$, and $p_1(s)$ is defined as follows

$$p_1(s) \triangleq \frac{1}{2}(s-1)^2 \tag{6}$$

where s=|∇∅|⩾0, and in the following, all of the variables s represent |∇∅|.

In calculus of variations, the energy functional E(ø) can be minimized by the evolution equation of the gradient flow

$$\frac{\partial \varnothing}{\partial t} = -\frac{\partial E}{\partial \varnothing} \tag{7}$$

where ∂E/(∂ø) represents the Gateaux derivative of the energy functional E(ø).

According to the linearity of the Gateaux derivative and Eq.(4), we have

$$\frac{\partial E}{\partial \varnothing} = \frac{\partial E_m}{\partial \varnothing} + \mu \frac{\partial P}{\partial \varnothing} \tag{8}$$

From Eq.(7) and Eq.(8), we have

$$\frac{\partial \varnothing}{\partial t} = -\frac{\partial E_m}{\partial \varnothing} - \mu \frac{\partial P}{\partial \varnothing} \tag{9}$$

The gradient flow of the penalized energy μP(ø) as follows

$$\frac{\partial \varnothing}{\partial t} = \mu \cdot \mathrm{div}[(1 - \frac{1}{|\nabla \varnothing|})\nabla \varnothing] \tag{10}$$

Obviously, this is a heat diffusion equation, and its diffusion rate is as follows

$$r_1 = \mu(1 - \frac{1}{s}) \tag{11}$$

The diffusion of the heat diffusion equation takes place when s is not equal to 1, at this point, there are two possible cases for the diffusion rate:

For s > 1, r_1 is a positive real number, therefore, the forward diffusion will reduce |∇∅|.

For s < 1, r_1 is negative, so the backward diffusion will increase |∇∅|.

This is a forward-and-backward (FAB) diffusion, and it adaptive decreases or increase |∇∅| to force the LSF to be close to the SDF, therefore, the complex re-initialization procedures are avoided.

2.2.2 DRLSE2

In the literature [15], Li et al. proposed a double-well potential algorithm. At the same time, he replaced the penalty term with a distance regularization term. Eq.(6) has the unique minimum point at s=1, which attempts to maintain the LSF as a SDF in the entire domain, but it also brings an undesirable side effect to the LSF. To avoid this problem, he proposes a double-well potential function as follows

$$p_2(s) \triangleq \begin{cases} \frac{1}{(2\pi)^2}(1-\cos(2\pi s)), & if\ s \le 1 \\ \frac{1}{2}(s-1)^2, & if\ s \ge 1 \end{cases} \tag{12}$$

By calculus of variations, the gradient flow of the energy functional consisting of the double-well potential function is as follows

$$\frac{\partial \varnothing}{\partial t} = \begin{cases} \mu \cdot div\left[\frac{\sin(2\pi s)}{2\pi s}\nabla \varnothing\right]; & if\ s \le 1 \\ \mu \cdot div[(1 - \frac{1}{s})\nabla \varnothing]; & if\ s \ge 1 \end{cases} \tag{13}$$

Obviously, Eq.(13) is also a diffusion equation, the corresponding diffusion rate is shown in the following formula

$$r_2 = \begin{cases} \mu \frac{\sin(2\pi s)}{2\pi s}; & if\ s \le 1 \\ \mu(1 - \frac{1}{s}); & if\ s \ge 1 \end{cases} \tag{14}$$

r_2 has three possible cases:

For s > 1, r_2 is a positive number, therefore, the forward diffusion will reduce |∇∅|.

For (1/2)⩽ s <1, the diffusion rate r_2 is negative, so the backward diffusion will increase |∇∅|.

For s< (1/2), the diffusion rate r_2 is a positive, so the forward diffusion will reduce $|\nabla\varnothing|$.

2.2.3 DRLSE3

The document [19] states that the Taylor polynomial should, in general, first be used for calculation of trigonometric function. Therefore, he uses polynomial instead of trigonometric function to obtain the double-well potential function algorithm as follows

$$p_3(s) \triangleq \begin{cases} \frac{1}{2}s^2(s-1)^2 + \frac{1}{2}s^3(s-1)^3, & if\ s \le 1 \\ \frac{1}{2}(s-1)^2, & if\ s > 1 \end{cases} \tag{15}$$

Dividing the first derivative of above double-well potential function by the variable s gives the diffusion rate as follows

$$r_3 = \begin{cases} \mu\left[(s-1)(2s-1) + \frac{3}{2}s(2s-1)(s-1)^2\right], & if\ s \le 1 \\ \mu\left(1-\frac{1}{s}\right), & if\ s > 1 \end{cases} \tag{16}$$

2.2.4 C-DRLSE

Xie et al.[17] points out some shortcomings of the DRLSE1, such as, it produces many "peaks" and "valleys" in the regions far from zero level set. He proposed the following level set regularization term to substitute Eq.(10)

$$\frac{\partial\varnothing}{\partial t} = \mu\nabla\cdot(H_\varepsilon(|\nabla\varnothing|-1)\nabla\varnothing) \tag{17}$$

where $H\varepsilon(z) = [1+(2/\pi)\arctan(z/\varepsilon)]/2$, and the value of ε is 0.5 in this article, which is a fixed parameter. As a result, its diffusion rate is as follows

$$r_X = \mu[0.5 + \frac{1}{\pi}\arctan 2(s-1)] \tag{18}$$

2.2.5 LSE-RD

Recently, Zhang et al. proposed a LSE-RD algorithm for GACs that completely eliminated re-initialization process in LSE [18]. The novel active contour evolution equation shown below

$$\begin{cases} \frac{\partial\varnothing}{\partial t} = \varepsilon\Delta\varnothing - \frac{1}{\varepsilon}L(\varnothing) \\ \varnothing(x,y,t=0,\varepsilon) = \varnothing_0(x,y) \end{cases} \tag{19}$$

whereε > 0, is a small constant, Δ is the Laplacian operator, $\varnothing_0(x,y)$ is the initial LSF, and $L(\varnothing)=-F\delta(\varnothing)$.

3 Flexible Coefficient Distance Regularized Level Set Evolution (FC- DRLSE)

We propose a flexible coefficient distance regularized level set evolution eliminates re-initialization method for image segmentation, whose energy functional is as follows

$$E(\varnothing) = E_m(\varnothing) + R(\varnothing) \tag{20}$$

where $E_m(\varnothing)$ is a certain energy functional that drives the level set motion, and $R(\varnothing)$ is the energy functional of the flexible coefficient distance regularized term. We define $R(\varnothing)$ as follows

$$R(\varnothing) \triangleq \int p_F(|\nabla\varnothing|)\,dxdy \tag{21}$$

where $p_F(s)$ is defined as follows

$$p_F(s) \triangleq \begin{cases} \frac{1}{2}Vs^2(s-1)^2, & if\ s < 1 \\ \frac{1}{2}\mu(s-1)^2, & if\ s \ge 1 \end{cases} \tag{22}$$

where μ⩾0, and V is a piecewise constant, defined as follows

$$V = \begin{cases} \mu, & if\ s < \frac{1}{2} \\ v, & if\ s \ge \frac{1}{2} \end{cases} \tag{23}$$

where v is a real constant.

We can get the first derivative of $p_F(s)$ as

$$p_F^{'}(s)=\begin{cases} Vs(s-1)(2s-1), & if\, s<1 \\ \mu(s-1), & if\, s\geq 1 \end{cases} \tag{24}$$

Dividing this first derivative by the variable s gives the diffusion rate as follows

$$r_F=\begin{cases} V(s-1)(2s-1), & if\, s<1 \\ \mu\left(1-\frac{1}{s}\right), & if\, s\geq 1 \end{cases} \tag{25}$$

Again, we can get the second derivative of $p_F(s)$ as follows

$$p_F^{''}(s)=\begin{cases} V[1-6s(1-s)], & if\, s<1 \\ \mu, & if\, s\geq 1 \end{cases} \tag{26}$$

The gradient flow of the penalized energy R(∅) as follows

$$\frac{\partial\varnothing}{\partial t}=\mathrm{div}\left[r_F(s)\nabla\varnothing\right]=\begin{cases} V\cdot div[(s-1)(2s-1)\nabla\varnothing], & if\, s<1 \\ \mu\cdot div[\left(1-\frac{1}{s}\right)\nabla\varnothing], & if\, s\geq 1 \end{cases} \tag{27}$$

4 Experimental Results

In this section, we compare our FC- DRLSE algorithm with other re-initialization free level set algorithms, which mainly include C-DRLSE, LSE-RD, DRLSE1, DRLSE2 and DRLSE3. All of these algorithms use the classic GAC model. In all of the experiments below, we initialized the LSF as a binary step function, and these experiments were conducted in Matlab 2017b platform on a Hasee God of War notebook computer with Intel Core i7-4700MQ CPU and 8G RAM. Except as noted below, we set the parameter toε=1.5, c_0=2,$\Delta t=\Delta t_1$=5, $\mu=1/(5\Delta t)$ =0.04,Δt_2=0.2, andλ=5 by default.

The parameter αneeds different values depending on the images. After the segmentation algorithm converges, the algorithm is iterated five times with the parameter $\alpha = 0$ to avoid the slight deviation of the final active contour from the target boundary of the image due to the weighted area term.

In the figures below of the experimental results, unless otherwise stated, all the blue rectangles represent initialized zero level set curves, and the red curves represent the segmentation result curves of each algorithm.

4.1 Experiments with Coefficient v=μ

In order to further test the performance of each algorithm, we apply each algorithm in a real image with size of 321× 481. We can see from Fig.1 that the C-DRLSE and LSE-RD algorithms cause target boundary leakage, especially the LSE-RD algorithm, while the DRLSE-S algorithms and our FC-DRLSE algorithm can segment the image normally.

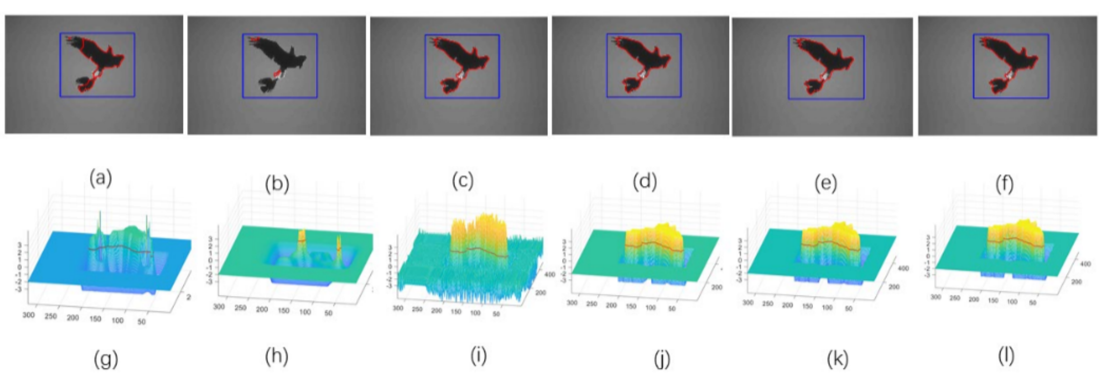

Figure 1 Segmentation results. (a)-(f) results obtained by C-DRLSE, LSE-RD, DRLSE1, DRLSE2, DRLSE3 and FC-DRLSE algorithm respectively. (g)-(l) 3D view of final LSF by C-DRLSE, LSE-RD, DRLSE1, DRLSE2, DRLSE3 and FC-DRLSE algorithm respectively

The red curves in Figure 1 are completely covered by the green curves, which means that the image segmentation results of the two algorithms are the same, that is to say, our FC-DRLSE algorithm is equivalent to the DRLSE2 algorithm in image segmentation results. The results of the competitive algorithms in the experiments above are consistent.

The above experiments, only the DRLSE2 algorithm, the DRLSE3 algorithm and the FC-DRLSE algorithm have no problem, then we compare the efficiency of these three algorithms. We repeat each of the above two experiments ten times to obtain the average running time of each algorithm as shown in Table 1.

As can be seen in Table 1, the DRLSE2 algorithm is the slowest algorithm, the DRLSE3 algorithm runs faster than the DRLSE2 algorithm, and the FC-DRLSE algorithm runs slightly faster than the DRLSE3 algorithm.

Table 1 Running Time

Algorithm	The running time of the first experiment	The running time of the second experiments
DRLSE2	0.8756	11.0143
DRLSE3	0.8209	10.9322
FC-DRLSE	0.8134	10.9179

The two experiments of this section show that:

(1) The DRLSE-S algorithms and our FC-DRLSE algorithm have better boundary anti-leakage ability than the C-DRLSE and the LSE-RD algorithms, and the LSE-RD algorithm is more prone to boundary leakage than the C-DRLSE algorithm;

(2) The FC-DRLSE algorithm and the DRLSE2 algorithm are almost equivalent in image segmentation, but the FC-DRLSE algorithm runs slightly faster, so our FC-DRLSE algorithm can replace the DRLSE2 algorithm completely.

4.2 Experiments with Coefficient v>>μ

The next three experiments will verify that our FC-DRLSE algorithm is more robust boundary anti-leakage than the DRLSE-S algorithms.

In the following two experiments, the parameters v be set to 8μ and 7μ , respectively, and the parameters α be successively 3.5 and 1.6.

Figure 2 and Figure 3, respectively, are the results of the above competing algorithms iterated 250 times for a real image and 250 times for a composite image.

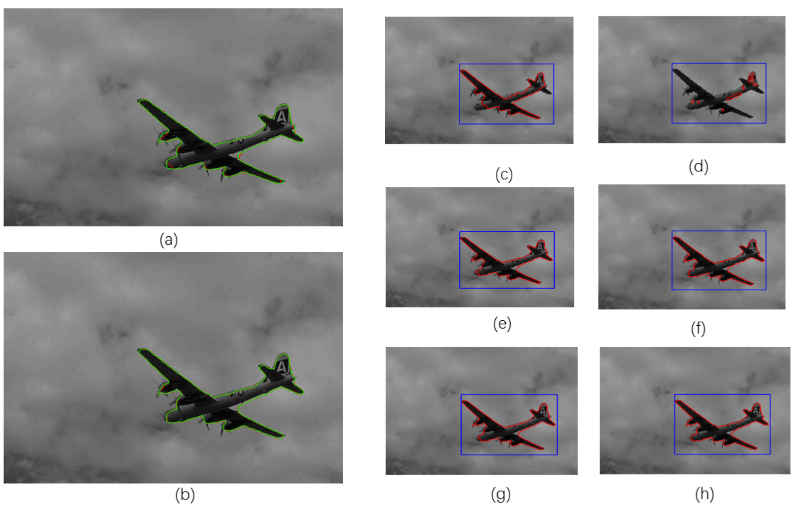

Figure 2 Segmentation results. (c)-(h) results obtained by C-DRLSE, LSE-RD, DRLSE1, DRLSE2, DRLSE3 and FC-DRLSE respectively. The red curves in (a) and (b) are the segmentation results by DRLSE2 and DRLSE1 respectively. The green curves in (a)(b) are the segmentation results by FC-DRLSE

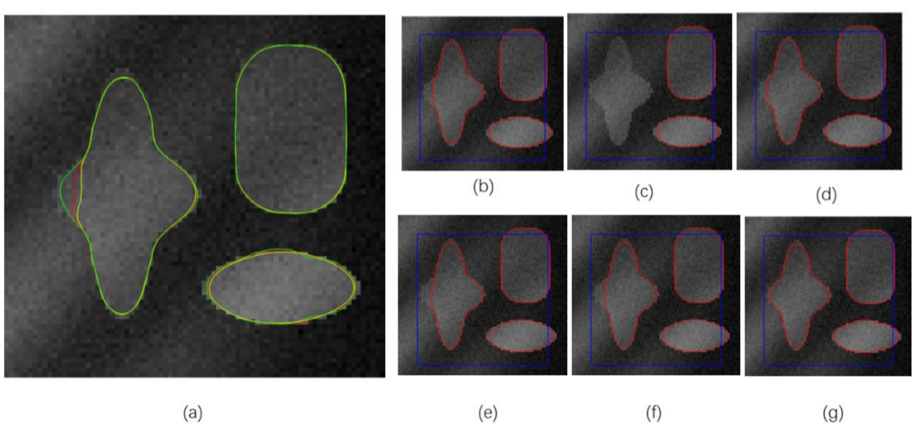

Figure3 Segmentation results. (b)-(g) results obtained by C-DRLSE, LSE-RD, DRLSE1, DRLSE2, DRLSE3 and FC-DRLSE respectively. The yellow curves, the red curves and the green curves in (a) are the segmentation results by DRLSE2, DRLSE1 and FC-DRLSE respectively

From Figure 2(c) - (h) and Figure 3(b) - (g), we can see that both the C-DRLSE algorithm and the LSE-RD algorithm generate serious boundary leaks, especially the LSE-RD algorithm. However, neither the DRLSE-S algorithm nor our FC-

DRLSE algorithm generates any serious boundary leakage, especially our FC-DRLSE algorithm.

The red curves in Figure 2(a) and Figure 2(b) are the image segmentation results of the DRLSE2 algorithm and the DRLSE1 algorithm respectively, and the green curves are the segmentation results of the FC-DRLSE algorithm. In Figure 2 (a), the DRLSE2 algorithm has significant boundary leakage compared to the FC-DRLSE algorithm. In Fig.2(b), the DRLSE1 algorithm has no obvious boundary leakage, but the red curves are all included in the green curves, it can be seen that the FC-DRLSE algorithm has slightly better boundary anti-leakage performance than the DRLSE1 algorithm.

The green curve, the red curve and the yellow curve in Figure 3(a) are the segmentation results of the FC-DRLSE algorithm, the DRLSE1 algorithm and the DRLSE2 algorithm, respectively. From the leftward boundary leakage in Figure 3 (a), we can see that the order from strong to weak in terms of boundary anti-leakage ability are the FC-DRLSE algorithm, the DRLSE1 algorithm and the DRLSE2 algorithm.

5 Conclusions

In this paper, we proposed a flexible coefficient distance regularized level set evolution without re-initialization algorithm, which uses different coefficients for the newly added energy functional term in different regions, so that this evolve rate of the LSF and image segmentation performance can be reconciled. After our research and exploration, we divide the coefficient v into three cases:(1) The case of the coefficient $v = \mu$. In this case, our FC-DRLSE algorithm and the DRLSE2 algorithm are almost equivalent in image segmentation ability, but the FC-DRLSE runs slightly faster. (2) The case of the coefficient $v >> \mu$. In this case, our FC-DRLSE algorithm has superb boundary anti-leakage ability. Although we divide the coefficient v roughly into two cases in this way, small variations of the coefficient v may have slight differences on the performance of the algorithm. Therefore, we suggest that the value of coefficient v should be different according to the actual situation. So the coefficient v is a flexible coefficient.

References

[1] Osher, S. and J.A. Sethian, Fronts propagating with curvature-dependent speed: Algorithms based on Hamilton-Jacobi formulations. Journal of Computational Physics. 79(1): p. 12-49 (1988).

[2] Kass M., A. Witkin and D. Terzopoulos, Snakes: Active contour models. International Journal of Computer Vision, 1988. 1(4): p. 321–331.

[3] Caselles V., R. Kimmel and G. Sapiro, Geodesic active contours. INTERNATIONAL JOURNAL OF COMPUTER VISION, 1997. 22(1): p. 61-79.

[4] Osher, S. and J.A. Sethian, Fronts propagating with curvature-dependent speed: Algorithms based on Hamilton-Jacobi formulations. Journal of Computational Physics, 1988. 79(1): p. 12-49.

[5] Malladi R., J.A. Sethian and B.C. Vemuri, Shape modeling with front propagation: a level set approach. IEEE Transactions on Pattern Analysis and Machine Intelligence, 1995. 17; 17(2; 2): p. 158-175.

[6] Peng D., et al., A PDE-Based Fast Local Level Set Method. Journal of Computational Physics, 1999. 155(2): p. 410-438.

[7] Weickert, J. and G. Kühne, Fast methods for implicit active contour models. *in Geometric Level Set Methods in Imaging,* Vision and Graphics, S. Osher and N. Paragios, Eds. New York: Springer-Verlag, 2003.

[8] Zhao H., et al., A Variational Level Set Approach to Multiphase Motion. Journal of Computational Physics, 1996. 127(1): p. 179-195.

[9] Vemuri, B. and Y. Chen, Joint Image Registration and Segmentation. Geometric Level Set Methods in Imaging, Vision, and Graphics, Springer, pp. 251-269, 2003.

[10] Chan, T.F. and L.A. Vese, Active contours without edges. IEEE Transactions on Image Processing, 2001. 10; 10(2; 2): p. 266-277.

[11] G.Aubert, and P. Kornprobst, Mathematical Problems in Image Processing. New York: Springer-Verlag, 2000

[12] J. A. Sethian, Level Set Methods and Fast Marching Methods, Cambridge: Cambridge University Press, 1999

[13] Osher, S. and R. Fedkiw, Level Set Methods and Dynamic Implicit Surfaces. New York: Springer-Verlag, 2002.

[14] Sussman M., P. Smereka and S. Osher, A Level Set Approach for Computing Solutions to Incompressible Two-Phase Flow. Journal of Computational Physics, 1994. 114(1): p. 146-159.

[15] Li C., et al., Distance Regularized Level Set Evolution and Its Application to Image Segmentation. IEEE Transactions on Image Processing, 2010. 19; 19(12; 12): p. 3243-3254.

[16] Li C., et al., Level set evolution without re-initialization: a new variational formulation, in 2005 IEEE Computer Society Conference on Computer Vision and Pattern Recognition (CVPR'05). 2005. p. 430-436 vol. 1.

[17] Xie X., Active Contouring Based on Gradient Vector Interaction and Constrained Level Set Diffusion. IEEE Transactions on Image Processing, 2010. 19; 19(1; 1): p. 154-164.

[18] Zhang K., et al., Reinitialization-Free Level Set Evolution via Reaction Diffusion. IEEE Transactions on Image Processing, 2013. 22; 22(1; 1): p. 258-271.

[19] Wang X., et al., A novel level set method for image segmentation by incorporating local statistical analysis and global similarity measurement. PATTERN RECOGNITION, 2015. 48(1): p. 189-204.